

An upper limit on the anomalous magnetic moment of the τ lepton

The OPAL Collaboration

Abstract

Using radiative $Z^0 \rightarrow \tau^+\tau^-\gamma$ events collected with the OPAL detector at LEP at $\sqrt{s} = M_Z$ during 1990–95, a direct study of the electromagnetic current at the $\tau\gamma$ vertex has been performed in terms of the anomalous magnetic form factor F_2 of the τ lepton. The analysis is based on a data sample of 1429 $e^+e^- \rightarrow \tau^+\tau^-\gamma$ events which are examined for a deviation from the expectation with $F_2 = 0$. From the non-observation of anomalous $\tau^+\tau^-\gamma$ production a limit of

$$-0.068 < F_2 < 0.065$$

is obtained. This can also be interpreted as a limit on the electric dipole form factor F_3 as

$$-3.8 \times 10^{-16} e \text{ cm} < eF_3 < 3.6 \times 10^{-16} e \text{ cm} .$$

The above ranges are valid at the 95% confidence level.

(Submitted to Physics Letters B)

The OPAL Collaboration

K. Ackerstaff⁸, G. Alexander²³, J. Allison¹⁶, N. Altekamp⁵, K.J. Anderson⁹,
S. Anderson¹², S. Arcelli², S. Asai²⁴, S.F. Ashby¹, D. Axen²⁹, G. Azuelos^{18,a},
A.H. Ball¹⁷, E. Barberio⁸, R.J. Barlow¹⁶, R. Bartoldus³, J.R. Batley⁵,
S. Baumann³, J. Bechtluft¹⁴, T. Behnke⁸, K.W. Bell²⁰, G. Bella²³, S. Bentvelsen⁸,
S. Bethke¹⁴, S. Betts¹⁵, O. Biebel¹⁴, A. Biguzzi⁵, S.D. Bird¹⁶, V. Blobel²⁷,
I.J. Bloodworth¹, M. Bobinski¹⁰, P. Bock¹¹, D. Bonacorsi², M. Boutemur³⁴,
S. Braibant⁸, L. Brigliadori², R.M. Brown²⁰, H.J. Burckhart⁸, C. Burgard⁸,
R. Bürgin¹⁰, P. Capiluppi², R.K. Carnegie⁶, A.A. Carter¹³, J.R. Carter⁵,
C.Y. Chang¹⁷, D.G. Charlton^{1,b}, D. Chrisman⁴, P.E.L. Clarke¹⁵, I. Cohen²³,
J.E. Conboy¹⁵, O.C. Cooke⁸, C. Couyoumtzelis¹³, R.L. Coxe⁹, M. Cuffiani²,
S. Dado²², C. Dallapiccola¹⁷, G.M. Dallavalle², R. Davis³⁰, S. De Jong¹², L.A. del
Pozo⁴, A. de Roeck⁸, K. Desch⁸, B. Dienes^{33,d}, M.S. Dixit⁷, M. Doucet¹⁸,
E. Duchovni²⁶, G. Duckeck³⁴, I.P. Duerdoth¹⁶, D. Eatough¹⁶, P.G. Estabrooks⁶,
E. Etzion²³, H.G. Evans⁹, M. Evans¹³, F. Fabbri², A. Fanfani², M. Fantì²,
A.A. Faust³⁰, L. Feld⁸, F. Fiedler²⁷, M. Fierro², H.M. Fischer³, I. Fleck⁸,
R. Folman²⁶, D.G. Fong¹⁷, M. Foucher¹⁷, A. Fürtjes⁸, D.I. Futyan¹⁶, P. Gagnon⁷,
J.W. Gary⁴, J. Gascon¹⁸, S.M. Gascon-Shotkin¹⁷, N.I. Geddes²⁰,
C. Geich-Gimbel³, T. Geralis²⁰, G. Giacomelli², P. Giacomelli⁴, R. Giacomelli²,
V. Gibson⁵, W.R. Gibson¹³, D.M. Gingrich^{30,a}, D. Glenzinski⁹, J. Goldberg²²,
M.J. Goodrick⁵, W. Gorn⁴, C. Grandi², E. Gross²⁶, J. Grunhaus²³, M. Gruwé²⁷,
C. Hajdu³², G.G. Hanson¹², M. Hansroul⁸, M. Hapke¹³, C.K. Hargrove⁷,
P.A. Hart⁹, C. Hartmann³, M. Hauschild⁸, C.M. Hawkes⁵, R. Hawkings²⁷,
R.J. Hemingway⁶, M. Herndon¹⁷, G. Herten¹⁰, R.D. Heuer⁸, M.D. Hildreth⁸,
J.C. Hill⁵, S.J. Hillier¹, P.R. Hobson²⁵, A. Hocker⁹, R.J. Homer¹, A.K. Honma^{28,a},
D. Horváth^{32,c}, K.R. Hossain³⁰, R. Howard²⁹, P. Hüntemeyer²⁷, D.E. Hutchcroft⁵,
P. Igo-Kemenes¹¹, D.C. Imrie²⁵, K. Ishii²⁴, A. Jawahery¹⁷, P.W. Jeffreys²⁰,
H. Jeremie¹⁸, M. Jimack¹, A. Joly¹⁸, C.R. Jones⁵, M. Jones⁶, U. Jost¹¹,
P. Jovanovic¹, T.R. Junk⁸, J. Kanzaki²⁴, D. Karlen⁶, V. Kartvelishvili¹⁶,
K. Kawagoe²⁴, T. Kawamoto²⁴, P.I. Kayal³⁰, R.K. Keeler²⁸, R.G. Kellogg¹⁷,
B.W. Kennedy²⁰, J. Kirk²⁹, A. Klier²⁶, S. Kluth⁸, T. Kobayashi²⁴, M. Kobel¹⁰,
D.S. Koetke⁶, T.P. Kokott³, M. Kolrep¹⁰, S. Komamiya²⁴, R.V. Kowalewski²⁸,
T. Kress¹¹, P. Krieger⁶, J. von Krogh¹¹, P. Kyberd¹³, G.D. Lafferty¹⁶,
R. Lahmann¹⁷, W.P. Lai¹⁹, D. Lanske¹⁴, J. Lauber¹⁵, S.R. Lautenschlager³¹,
I. Lawson²⁸, J.G. Layter⁴, D. Lazic²², A.M. Lee³¹, E. Lefebvre¹⁸, D. Lellouch²⁶,
J. Letts¹², L. Levinson²⁶, B. List⁸, S.L. Lloyd¹³, F.K. Loebinger¹⁶, G.D. Long²⁸,
M.J. Losty⁷, J. Ludwig¹⁰, D. Lui¹², A. Macchiolo², A. Macpherson³⁰,
M. Mannelli⁸, S. Marcellini², C. Markopoulos¹³, C. Markus³, A.J. Martin¹³,
J.P. Martin¹⁸, G. Martinez¹⁷, T. Mashimo²⁴, P. Mättig²⁶, W.J. McDonald³⁰,
J. McKenna²⁹, E.A. Mckigney¹⁵, T.J. McMahon¹, R.A. McPherson²⁸, F. Meijers⁸,
S. Menke³, F.S. Merritt⁹, H. Mes⁷, J. Meyer²⁷, A. Michelini², S. Mihara²⁴,

G. Mikenberg²⁶, D.J. Miller¹⁵, A. Mincer^{22,e}, R. Mir²⁶, W. Mohr¹⁰, A. Montanari²,
T. Mori²⁴, S. Mihara²⁴, K. Nagai²⁶, I. Nakamura²⁴, H.A. Neal¹², B. Nellen³,
R. Nisius⁸, S.W. O’Neale¹, F.G. Oakham⁷, F. Odorici², H.O. Ogren¹², A. Oh²⁷,
N.J. Oldershaw¹⁶, M.J. Oreglia⁹, S. Orito²⁴, J. Pálinkás^{33,d}, G. Pásztor³²,
J.R. Pater¹⁶, G.N. Patrick²⁰, J. Patt¹⁰, R. Perez-Ochoa⁸, S. Petzold²⁷,
P. Pfeifenschneider¹⁴, J.E. Pilcher⁹, J. Pinfold³⁰, D.E. Plane⁸, P. Poffenberger²⁸,
B. Poli², A. Posthaus³, C. Rembser⁸, S. Robertson²⁸, S.A. Robins²²,
N. Rodning³⁰, J.M. Roney²⁸, A. Rooke¹⁵, A.M. Rossi², P. Routenburg³⁰,
Y. Rozen²², K. Runge¹⁰, O. Runolfsson⁸, U. Ruppel¹⁴, D.R. Rust¹², K. Sachs¹⁰,
T. Saeki²⁴, O. Sahr³⁴, W.M. Sang²⁵, E.K.G. Sarkisyan²³, C. Sbarra²⁹,
A.D. Schaile³⁴, O. Schaile³⁴, F. Scharf³, P. Scharff-Hansen⁸, J. Schieck¹¹,
P. Schleper¹¹, B. Schmitt⁸, S. Schmitt¹¹, A. Schöning⁸, M. Schröder⁸,
M. Schumacher³, C. Schwick⁸, W.G. Scott²⁰, T.G. Shears⁸, B.C. Shen⁴,
C.H. Shepherd-Themistocleous⁸, P. Sherwood¹⁵, R.P.B. Sieberg³, G.P. Siroli²,
A. Sittler²⁷, A. Skillman¹⁵, A. Skuja¹⁷, A.M. Smith⁸, G.A. Snow¹⁷, R. Sobie²⁸,
S. Söldner-Rembold¹⁰, R.W. Springer³⁰, M. Sproston²⁰, K. Stephens¹⁶,
J. Steuerer²⁷, B. Stockhausen³, K. Stoll¹⁰, D. Strom¹⁹, R. Ströhmer³⁴,
P. Szymanski²⁰, R. Tafirout¹⁸, S.D. Talbot¹, P. Taras¹⁸, S. Tarem²², R. Teuscher⁸,
M. Thiergen¹⁰, M.A. Thomson⁸, E. von Törne³, E. Torrence⁸, S. Towers⁶,
I. Trigger¹⁸, Z. Trócsányi³³, E. Tsur²³, A.S. Turcot⁹, M.F. Turner-Watson⁸,
I. Ueda²⁴, P. Utzat¹¹, R. Van Kooten¹², P. Vannerem¹⁰, M. Verzocchi¹⁰,
P. Vikas¹⁸, E.H. Vokurka¹⁶, H. Voss³, F. Wäckerle¹⁰, A. Wagner²⁷, C.P. Ward⁵,
D.R. Ward⁵, P.M. Watkins¹, A.T. Watson¹, N.K. Watson¹, P.S. Wells⁸,
N. Vermes³, J.S. White²⁸, G.W. Wilson²⁷, J.A. Wilson¹, T.R. Wyatt¹⁶,
S. Yamashita²⁴, G. Yekutieli²⁶, V. Zacek¹⁸, D. Zer-Zion⁸

¹School of Physics and Astronomy, University of Birmingham, Birmingham B15 2TT, UK

²Dipartimento di Fisica dell’ Università di Bologna and INFN, I-40126 Bologna, Italy

³Physikalisches Institut, Universität Bonn, D-53115 Bonn, Germany

⁴Department of Physics, University of California, Riverside CA 92521, USA

⁵Cavendish Laboratory, Cambridge CB3 0HE, UK

⁶Ottawa-Carleton Institute for Physics, Department of Physics, Carleton University, Ottawa, Ontario K1S 5B6, Canada

⁷Centre for Research in Particle Physics, Carleton University, Ottawa, Ontario K1S 5B6, Canada

⁸CERN, European Organisation for Particle Physics, CH-1211 Geneva 23, Switzerland

⁹Enrico Fermi Institute and Department of Physics, University of Chicago, Chicago IL 60637, USA

¹⁰Fakultät für Physik, Albert Ludwigs Universität, D-79104 Freiburg, Germany

¹¹Physikalisches Institut, Universität Heidelberg, D-69120 Heidelberg, Germany

¹²Indiana University, Department of Physics, Swain Hall West 117, Bloomington IN 47405, USA

¹³Queen Mary and Westfield College, University of London, London E1 4NS, UK

¹⁴Technische Hochschule Aachen, III Physikalisches Institut, Sommerfeldstrasse 26-28, D-52056 Aachen, Germany

¹⁵University College London, London WC1E 6BT, UK

¹⁶Department of Physics, Schuster Laboratory, The University, Manchester M13 9PL, UK

¹⁷Department of Physics, University of Maryland, College Park, MD 20742, USA

¹⁸Laboratoire de Physique Nucléaire, Université de Montréal, Montréal, Quebec H3C 3J7, Canada

¹⁹University of Oregon, Department of Physics, Eugene OR 97403, USA

²⁰Rutherford Appleton Laboratory, Chilton, Didcot, Oxfordshire OX11 0QX, UK

²²Department of Physics, Technion-Israel Institute of Technology, Haifa 32000, Israel

²³Department of Physics and Astronomy, Tel Aviv University, Tel Aviv 69978, Israel

²⁴International Centre for Elementary Particle Physics and Department of Physics, University of Tokyo, Tokyo 113, and Kobe University, Kobe 657, Japan

²⁵Institute of Physical and Environmental Sciences, Brunel University, Uxbridge, Middlesex UB8 3PH, UK

²⁶Particle Physics Department, Weizmann Institute of Science, Rehovot 76100, Israel

²⁷Universität Hamburg/DESY, II Institut für Experimental Physik, Notkestrasse 85, D-22607 Hamburg, Germany

²⁸University of Victoria, Department of Physics, P O Box 3055, Victoria BC V8W 3P6, Canada

²⁹University of British Columbia, Department of Physics, Vancouver BC V6T 1Z1, Canada

³⁰University of Alberta, Department of Physics, Edmonton AB T6G 2J1, Canada

³¹Duke University, Dept of Physics, Durham, NC 27708-0305, USA

³²Research Institute for Particle and Nuclear Physics, H-1525 Budapest, P O Box 49, Hungary

³³Institute of Nuclear Research, H-4001 Debrecen, P O Box 51, Hungary

³⁴Ludwigs-Maximilians-Universität München, Sektion Physik, Am Coulombwall 1, D-85748 Garching, Germany

^a and at TRIUMF, Vancouver, Canada V6T 2A3

^b and Royal Society University Research Fellow

^c and Institute of Nuclear Research, Debrecen, Hungary

^d and Department of Experimental Physics, Lajos Kossuth University, Debrecen,
Hungary

^e and Department of Physics, New York University, NY 1003, USA

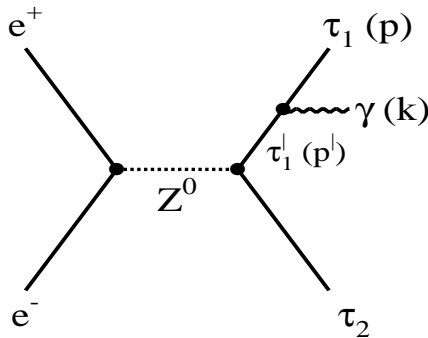
Introduction

Measurements of the anomalous magnetic moment of the electron [1] and the muon [2] by spin precession methods are considered the most precise tests of Quantum Electrodynamics (QED) and are usually expressed in terms of a deviation of their respective g -factors from the value of two [3]

$$a_e = \left(\frac{g_e - 2}{2} \right) = (1159.652193 \pm 0.000010) \times 10^{-6} \quad , \quad (1)$$

$$a_\mu = \left(\frac{g_\mu - 2}{2} \right) = (1165.9230 \pm 0.0084) \times 10^{-6} \quad . \quad (2)$$

Due to the τ lepton's short lifetime of $(291.0 \pm 1.5) \times 10^{-15}$ s, its anomalous magnetic moment cannot in practice be measured by a spin precession method and no direct measurement of a_τ exists so far. While the hadronic and weak contributions to a_e are very small, they are no longer negligible for a_μ and a_τ . A theoretical prediction for a_τ , based purely on QED, is $(1173.19 \pm 0.01) \times 10^{-6}$ [4]. Additional weak and strong contributions [4, 5] modify this to $(1177.3 \pm 0.3) \times 10^{-6}$. Using the total width of $Z^0 \rightarrow \tau^+ \tau^-$, ref. [6] indirectly derives an upper limit on a_τ of $|a_\tau| < 0.01$ at 95% confidence level.



In order to constrain a_τ as suggested by Grifolz and Mendez [7], we have studied the process $e^+e^- \rightarrow \tau^+\tau^-\gamma$ in which a final-state photon is radiated from one of the tau leptons, as shown in the Feynman diagram above. The electromagnetic current of a fermion with mass m and charge e can be written using the general form factor decomposition

$$j_{\text{em}}^\mu = e\bar{u}(p') \left[\gamma^\mu F_1(q^2) + \frac{i}{2m} F_2(q^2) \sigma^{\mu\nu} q_\nu + \gamma^5 \sigma^{\mu\nu} q_\nu F_3(q^2) \right] u(p), \quad (3)$$

with p', p being the four-momenta of the τ lepton before and after the emission of the photon with four-momentum q and $q^2 = (p - p')^2$. At $q^2 = 0$, $F_1(0) = 1$

while $F_2(0) = a_f$, and $eF_3(0) = d_\tau^{\text{el}}$ define the anomalous magnetic and electric dipole moment, respectively. Note that the Standard Model predicts $F_3 = 0$.

However, this ansatz is not directly applicable to the $\tau' \rightarrow \tau\gamma$ vertex in $e^+e^- \rightarrow \tau^+\tau^-\gamma$, since the τ' , which emits the photon, is off-shell. Instead, the pertinent part of the amplitude must be written as

$$\frac{i(\not{p}' + m)}{p'^2 - m^2} ie \left[\gamma^\mu F_1(p'^2, q^2) + \frac{i}{2m} F_2(p'^2, q^2) \sigma^{\mu\nu} q_\nu + \gamma^5 \sigma^{\mu\nu} q_\nu F_3(p'^2, q^2) \right] \epsilon(\kappa) u(p) \quad . \quad (4)$$

The photon belongs to the final state, so it is real and therefore $F_2(p'^2, q^2)$ is measured at $q^2 = 0$, but averaged over a range of p'^2 from m_τ^2 to $(M_Z - m_\tau)^2$. In this analysis the minimum value of p'^2 after the event selection is $(13 \text{ GeV})^2$.

In this paper we search for an excess in the production of $e^+e^- \rightarrow \tau^+\tau^-\gamma$ events due to a non-vanishing form factor $F_2(p'^2, 0)$ as defined by eq. (4), assuming that $F_3 = 0$. Differential photon rates are compared to Monte Carlo predictions for the standard F_1 and the anomalous F_2 term. The extracted bound on the number of excess events from the F_2 term is used to determine an upper limit on F_2 averaged over p'^2 . Henceforth this interpretation of F_2 is always implied. Conversely, assuming $F_2 = 0$ a limit on F_3 is obtained. Because the sensitivity of this analysis is not sufficient to measure a value of F_2 as small as predicted [4] by the Standard Model (SM), the reported results mainly address new physics phenomena beyond the SM. Such phenomena may occur in the context of composite τ leptons [8], leptoquark models [9], or in models in which the electroweak symmetry breaking is driven by the third quark and lepton generation such as top-condensation or top-colour models [10].

It should be noted that the ansatz of eq. (4) can parametrize modifications of only the $\tau' \rightarrow \tau\gamma$ vertex. Radiative corrections involving both final-state taus, as well as the non-vanishing p'^2 , therefore limit a direct interpretation of F_2 in terms of the τ -lepton's anomalous magnetic moment $a_\tau = F_2(0, 0)$. For physics beyond the SM at an interaction scale $\Lambda_{\text{new}} \gg M_Z$, however, there is no such limitation in the above ansatz. In fact, as long as $|p'^2 - m_\tau^2| \ll \Lambda_{\text{new}}^2$, equating F_2 with the a_τ pertaining to the new interaction is correct.

The calculation which is used here to predict the distribution of photons arising from the different contributions assumes no interference between the F_1 and the F_2 term. The interference term is suppressed by m_τ^2/M_Z^2 . No severe restriction is imposed by this assumption for the precision of the F_2 measurement described below. Modifications of the results due to the interference term are treated at the end of the paper.

Monte Carlo simulation

The Monte Carlo simulation of the process $e^+e^- \rightarrow \tau^+\tau^-\gamma$ with $F_2 = F_3 = 0$ is provided by the program KORALZ [11] including initial (ISR) and final (FSR) state photon radiation up to $\mathcal{O}(\alpha^2)$. To the extent that the expectation for F_2 within the SM is small compared to the sensitivity of this analysis, KORALZ is assumed to represent the SM expectation throughout this paper. The τ decay is simulated by the TAUOLA [12] package which includes photon radiation from the leptonic decay products up to $\mathcal{O}(\alpha)$ and also from hadronic decay products using the program package PHOTOS [13]. According to studies using the KORALZ MC, the only source of photons contributing to the selected events studied in this analysis will be from ISR and FSR. Photons from π^0 decays do not enter as background to this analysis after the event selection.

The contribution of $\tau^+\tau^-\gamma$ events coming from a non-vanishing form factor F_2 is simulated using a calculation by Zeppenfeld [15] based on the F_2 term in eq.(4), assuming $m_\tau = 0$ and neglecting interference. The resulting differential cross section is given in the Appendix. In fact, the approximation of $m_\tau = 0$ implies a chirality (=helicity) flip in the amplitude for the F_2 contribution, while the Standard Model radiation always conserves chirality. As a result, there is no interference between the Standard Model and the F_2 contribution in the massless limit. Conversely, the size of the interference term then checks the validity of the $m_\tau = 0$ approximation. A very recent calculation [16] of radiative tau pair production through anomalous electromagnetic couplings including interference effects and a finite τ mass confirms the validity of the assumptions ($m_\tau = 0$, interference neglected) made here. Ref.[16] concludes that anomalous contributions from initial-state final-state interference, Z^0/γ interference and γ exchange can also be safely neglected.

Events generated from both the F_1 bremsstrahlung term (KORALZ) and the F_2 contribution are processed through a full simulation of the OPAL detector [14]. For the purpose of the efficiency determination for the F_2 contribution (signal), events have been generated by KORALZ and selected according to the 5-dimensional differential F_2 cross section (see Appendix) employing a ‘hit or miss’ method.

Figure 1 shows comparisons of the anomalous contribution and the KORALZ prediction in simulated distributions of the energy of the radiated photon E_γ (a), the acollinearity angle θ_{acol} between the τ lepton directions (b), and the emission angle of the photon with respect to the beam direction $\cos \theta_\gamma$ (c). Note, that the anomalous part is arbitrarily normalized. The striking difference between the distributions suggests that these variables are useful discriminators for this analysis: F_2 photons appear to be preferentially at high energies and are emitted

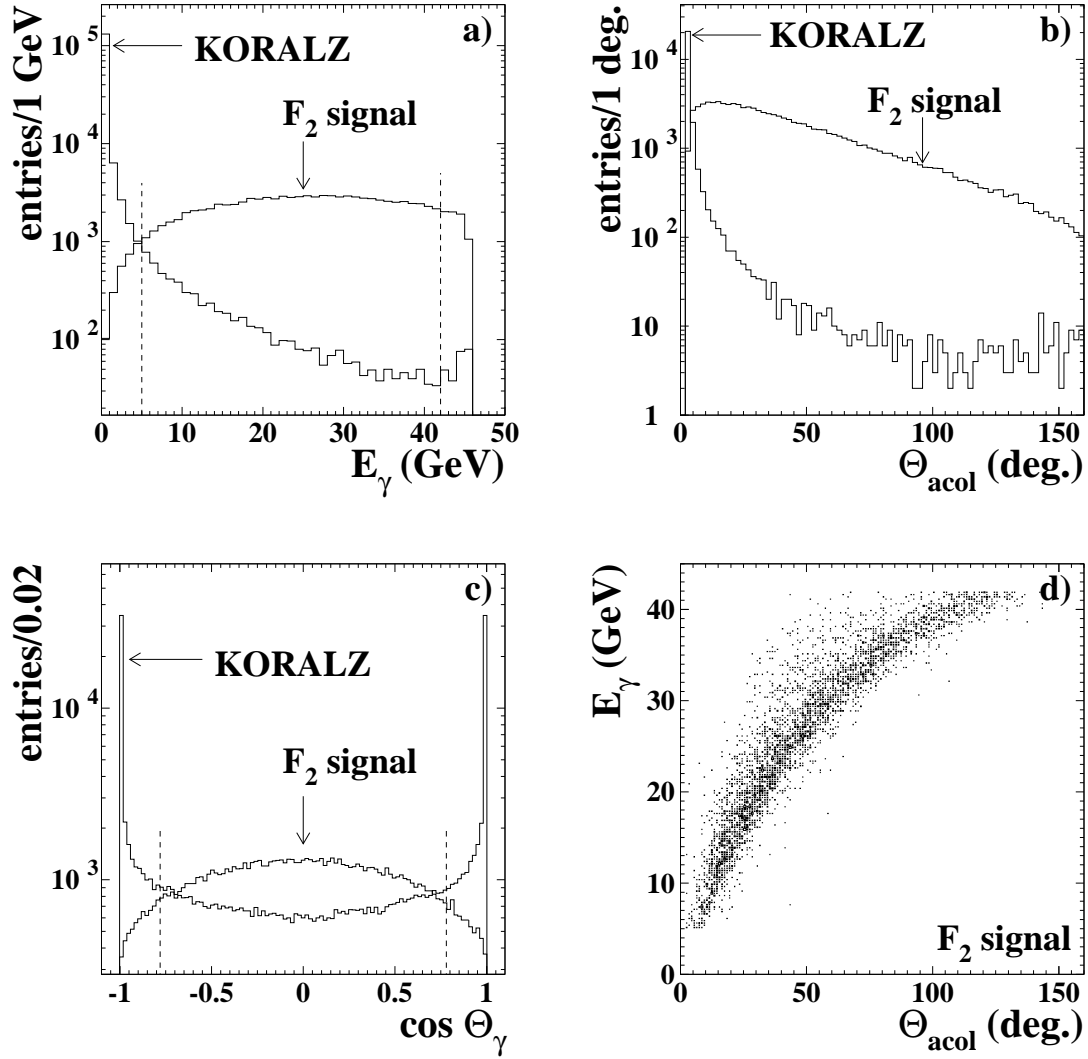


Figure 1: Comparison between the F_2 signal and the Standard Model expectation represented by KORALZ. (a) the photon energy E_γ , (b) the acollinearity angle θ_{acol} of the τ leptons and (c) the photon angle $\cos \theta_\gamma$ w.r.t. the beam direction. The relative normalization of the distributions is arbitrary, no detector effects are included. The dashed lines in (a) and (c) indicate the acceptance cuts. (d) photon energy E_γ vs. acollinearity angle for the F_2 signal prediction after full detector simulation.

at large angles to both τ 's. However, E_γ and θ_{acol} are strongly correlated (fig. 1 (d)), and the $\cos \theta_\gamma$ distribution is almost isotropic in an accepted θ_γ range with reduced background ($|\cos \theta_\gamma| < 0.78$). Consequently, the benefit obtained when using two-dimensional information in the above variables has been found to be marginal and also more sensitive to systematic effects. Therefore, in what follows only the photon energy distribution is used.

For the simulation of background processes the Monte Carlo generators [17] JETSET 7.4 ($q\bar{q}$), RADBAB 2.0 (e^+e^-), KORALZ 4.0 ($\mu^+\mu^-$) and VERMASEREN 1.01 (2γ) have been used.

Event Selection

For this analysis events recorded with the OPAL detector during the years 1990 to 1995 at a centre of mass energy $\sqrt{s} = M_Z$, corresponding to an integrated luminosity of about 180 pb^{-1} , have been used. 'Off-peak' data were not used to avoid deficiencies due to the lack of Z^0/γ interference effects in the signal MC. The number of produced τ pairs is about 230 000. The OPAL detector and its performance have been described elsewhere [18]. Isolated final-state photons are detected in the lead glass electromagnetic calorimeter covering an angular range in the barrel region of $|\cos \theta| < 0.81$ with an energy resolution of $\sigma_E/E \approx 12\%/\sqrt{E(\text{GeV})}$.

In selecting events containing τ pairs with an additional radiated photon, background is expected from e^+e^- , $\mu^+\mu^-$, multihadron, and two-photon events with any final state. Lepton pair events are selected by standard cuts [19] against $Z^0 \rightarrow q\bar{q}$ (cut on track and cluster multiplicity), two-photon processes (cut on visible energy) and cosmic ray background. The cut on the acollinearity of the τ pair is of course omitted in the preselection since it would also reject most of the signal events. Then e^+e^- and $\mu^+\mu^-$ events are recognized and rejected by high detected energy in the electromagnetic calorimeter (ECAL) or by high momentum tracks, low energy deposits in the calorimeters and μ chamber hits, respectively. The observed τ decay products are required to lie in a cone of half opening angle of 35° . We assume the τ flight direction to be identical with the cone axis, defined by the vector sum of the associated tracks and all neutral clusters. A $\tau^+\tau^-\gamma$ candidate event is selected if a photon candidate of at least 5 GeV and less than 42 GeV energy deposit is found outside both cones. The high energy cut is imposed to avoid the energy region where the $m_\tau = 0$ assumption in the F_2 MC has an impact on the E_γ distribution. To avoid losing τ decay products inside the beam pipe, $|\cos \theta_\tau| < 0.9$ has to be valid for both τ cones. A sample of 3 435 events survive this preselection.

Background from non- τ events is further reduced by the following requirements:

- to suppress initial state radiation the photon has to be in the barrel region of the detector ($|\cos \theta_\gamma| < 0.78$).
- to reject e^+e^- and $\mu^+\mu^-$ events, the visible energy or visible momentum of the more energetic τ candidate must be smaller than 35 GeV.
- the scalar sum of the momenta of the detected decay products of both tau candidates and the photon must be smaller than 75 GeV; furthermore events for which both τ cones are identified as $\tau \rightarrow \mu\nu\bar{\nu}$ decays are rejected. These cuts add to the suppression of $\mu^+\mu^-$ events.
- only events with 2 or 4 charged tracks (1-1 and 1-3 topologies) are retained.

The three-body final state of the signal process $e^+e^- \rightarrow \tau^+\tau^-\gamma$ is completely determined by two independent variables, i.e. the acollinearity angle between the τ leptons can be calculated from the measured photon energy E_γ and the measured angle between the photon and the τ^- . The measured acollinearity angle is required to agree within $\pm 50^\circ$ with the calculated angle. This cut greatly reduces multihadron background, two-photon events and incorrectly reconstructed events.

The above selection results in a total of 1429 $e^+e^- \rightarrow \tau^+\tau^-\gamma$ candidate events. The contribution of background from e^+e^- , $\mu^+\mu^-$ and multihadron events to this sample is estimated to total $(0.13 \pm 0.13)\%$.

Figure 2 shows the observed distribution of the measured photon energy for the selected events. Superimposed are the expectation from the Standard Model (KORALZ), normalized to the number of data events (shaded) and the distribution of F_2 -produced photons including full detector simulation (open histogram). In order to extract a limit on the F_2 form factor the data distribution of fig. 2 is fitted to a sum of both MC contributions using a binned likelihood \mathcal{L} assuming a Poisson distribution of the data events. In this fit the sum of both contributions has been normalized to the number of observed data events for each assumed value of F_2 . To test the method, we have performed fits to Monte Carlo event samples of the size of the data sample, using a 5% and a 10% F_2 contribution, respectively. In both cases the input values were reproduced (0.045 ± 0.010 and 0.096 ± 0.007 , respectively).

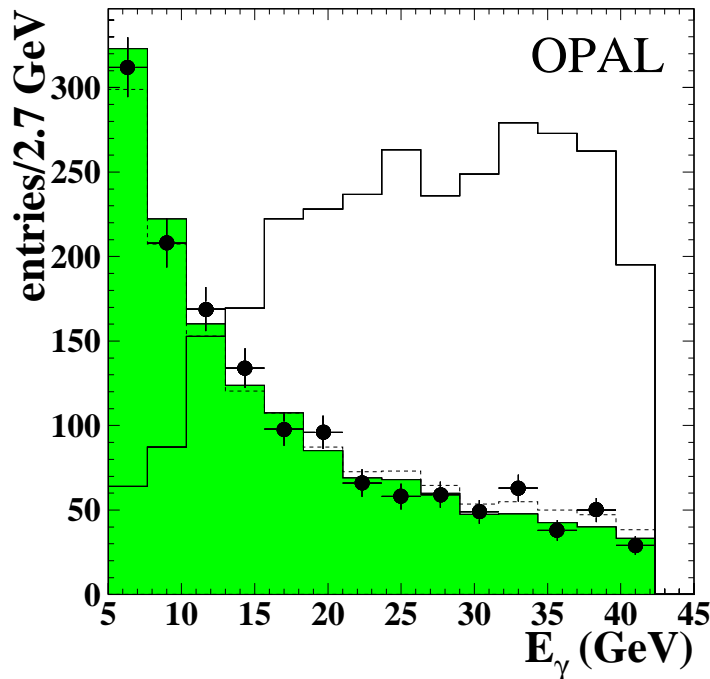


Figure 2: Photon energy spectra for data (points), KORALZ (shaded histogram, normalized to the data), and signal (open histogram, arbitrarily normalized). The dashed line shows the Monte Carlo prediction for $F_2 = 0.064$, also normalized to the data.

Fit Results

Figure 3(a) shows the dependence of the likelihood function on $|F_2|$. The most probable value is $|F_2| = 0.037$ which is offset from, but consistent with zero within about one standard deviation ($^{+0.015}_{-0.028}$) which is evident from the shallowness of the maximum of $\log\mathcal{L}$ in fig. 3(a). The 95% confidence level value is obtained from fig. 3(a) at the point where $\log\mathcal{L}$ has dropped by 1.92 units from its maximum as

$$|F_2| < 0.064 \quad \text{at} \quad 95\% \text{ C.L.} \quad (5)$$

The analysis has also been performed by normalizing the KORALZ MC to the integrated luminosity of the data. In this case the luminosity has been inferred from the total number of τ -pair events using the standard OPAL τ -pair selection. While intuitively one might expect a tighter constraint on $|F_2|$, the necessity to know the detection efficiency introduces an additional uncertainty not present

in the approach described above which is only sensitive to a difference in shape of the E_γ distribution between data and MC. Both effects have been tested (see section on systematic errors). When normalizing to the integrated luminosity the uncertainty of $\pm 6\%$ in the knowledge of the detection efficiency yields a limit on $|F_2|$ even slightly higher (0.065) than that obtained using the shape information only.

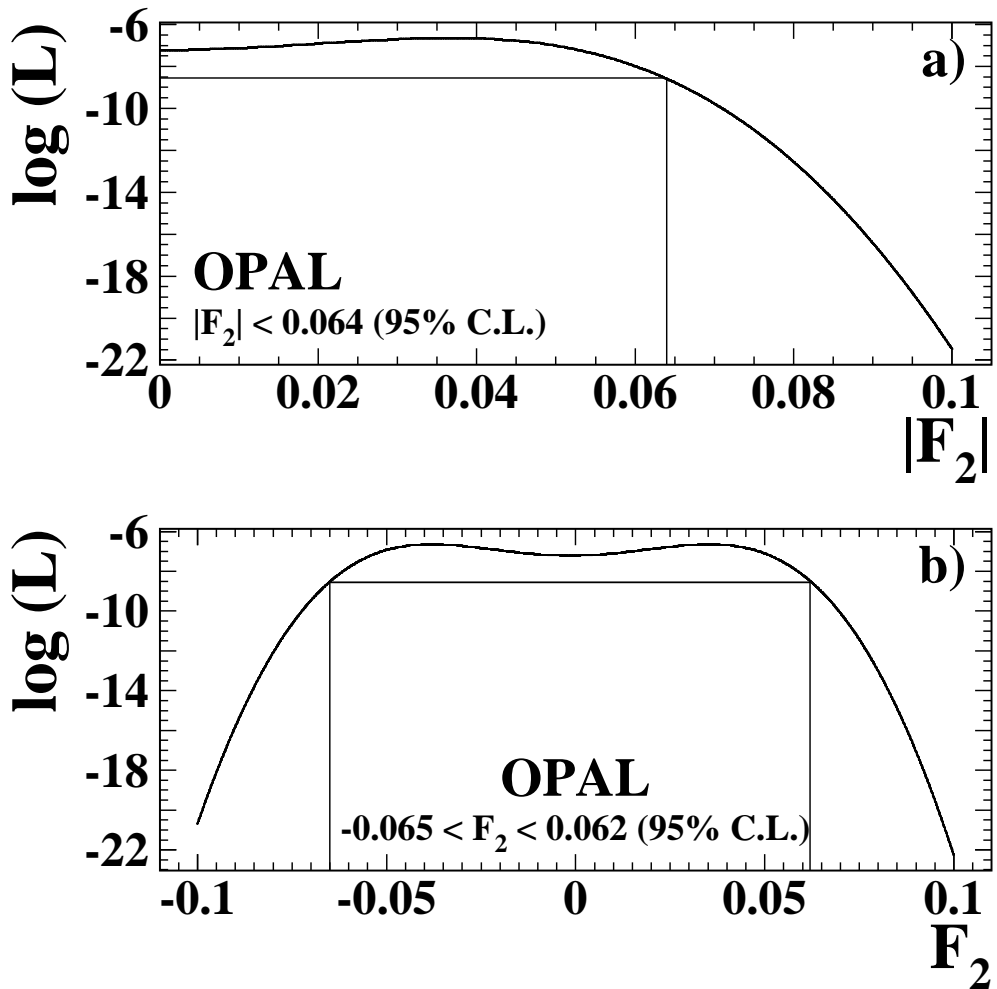


Figure 3: (a) Likelihood as a function of the fit parameter $|F_2|$. (b) Likelihood as a function of F_2 taking into account the interference term as described in the corresponding section of the text.

Systematic Errors

The systematic uncertainties due to the selection cuts, the photon detection efficiency, non- τ background, binning effects, Monte Carlo statistics and normalization, and the calibration uncertainty in the photon energy measurement have been studied. The omission of the interference term is discussed separately below.

Variations of the *selection cuts* indicate a systematic uncertainty on the limit on $|F_2|$ of about 0.005, the largest influence coming from varying the visible energy cut for the τ cone from 35 GeV to 32 GeV.

The effect of *binning* has been studied by varying the number of bins in the energy spectrum from 15 to 20 and by moving the bin boundaries by half a bin width. This leads to a maximum change in the limit on $|F_2|$ of +0.002.

The *photon energy calibration* has been investigated as a source of systematic error. The agreement in the energy measurement of the electromagnetic calorimeter between data and MC is better than 0.9%, determined from a comparison of π^0 invariant masses involving all photon energies. A systematic shift of the photon energy by this amount results in a systematic uncertainty on the limit on F_2 smaller than 0.001.

The uncertainty in the *description of the photon detection efficiency* and its dependence on the energy can make an important contribution to the systematic error of this analysis. An imperfect description of the efficiency would distort the photon energy spectrum and could thus lead to a bias for the resulting F_2 contribution. The quality of the efficiency simulation has been checked using the photon energy spectrum of radiative e^+e^- events where a high energy electron (> 43 GeV) has been required to tag the event in comparison with corresponding MC events. The efficiency ratio between data and MC is constant as a function of E_γ and consistent with unity to $\pm 6\%$. The resulting effect on the limit amounts to less than ± 0.0005 .

Background from non- τ events has been estimated using the MC simulation considering all background reactions mentioned above and is found to be very small (0.13%). The total predicted background from e^+e^- , $\mu^+\mu^-$, and hadronic processes amounts to 1.8 ± 1.8 events. The worst case assumption is that the background is distributed as the Standard Model expectation thereby artificially improving the limit. The resulting upper limit on F_2 , when the background is included, is however unchanged.

Because the MC event sample is about 4.5 times larger than the data we have neglected the *statistical error of the MC* in the fit. To check the validity of this

assumption, the fit has also been performed using a method [20] which allows for the inclusion of both data and MC error in the likelihood. The resulting limit changes negligibly by 0.0003 with respect to that obtained without using the MC error.

Assuming the systematic errors to be independent, they have been added in quadrature. Then the total systematic uncertainty has been quadratically added to the statistical error in each bin of the E_γ distribution and a new limit has been derived ¹ as

$$|F_2| < 0.067 \quad \text{at} \quad 95\% \text{ C.L.} \quad (6)$$

Inclusion of the Interference Term

It has been shown [21] for the cross section of the process $e^+e^- \rightarrow \tau^+\tau^-\gamma$ that the contribution of the interference between the standard part and the magnetic part of the electromagnetic current (see eq. (3)) can be important even if F_2 is as large as several percent. The authors of [21] have computed the differential cross section in the photon variables E_γ and $\cos \theta_\gamma$ for the $e^+e^- \rightarrow \tau^+\tau^-\gamma$ process including the interference term. While this computation cannot serve for event simulation by means of 4-vector generation, it has been used to study the relative importance of both terms.

Figure 4 shows the contribution of the interference term to the cross section assuming $|F_2| = 0.064$ for two different cuts on the event topology: without any requirement on the angular separation between the photon and the τ leptons (thin curves), and requiring a minimum angular separation of 35° (thick curves) as in this analysis. In each case, the central (solid) curve shows the cross section assuming an $|F_2|^2$ contribution only, while the upper/lower (dashed) curves are obtained by including the interference term with a positive/negative sign. It is evident that the effect of the interference term is much reduced by requiring a minimum angular separation between the photon and the τ leptons. Nevertheless, the effect of the interference term can be taken into account to obtain a limit on F_2 respecting its sign.

A correction of the signal spectrum is obtained by reweighting the signal E_γ spectrum according to fig. 4 using different weighting factors for each value of F_2 . Obviously, adding the interference term with a positive sign leads to a shift of the photon energy spectrum towards higher energies leading to an even better distinction between the SM and the F_2 spectrum, while for the negative sign the

¹Because the Poisson-based likelihood method does not have an explicit error term, χ^2 has been used for this estimation.

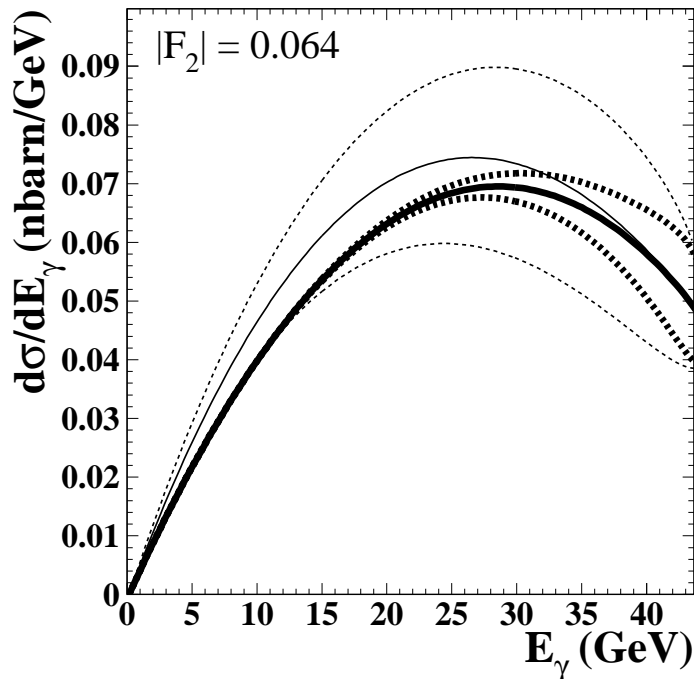


Figure 4: Influence of the interference term; the thin lines show the cross-section without any additional cuts applied (solid for the $|F_2|^2$ term alone and dashed with interference term included). The thick lines (solid and dashed, respectively) show the result when a minimum angle of 35° between the photon and the τ -cone axis is required.

opposite is true. This treatment assumes equal efficiencies for events due to the interference term and to the quadratic term, an assumption which is not entirely correct. However, as long as the efficiency for the interference term is not larger than that of the quadratic term, this assumption is conservative and is, in fact, supported by the angular distributions shown in fig. 1(c). The interference term distribution must lie in between KORALZ and the $|F_2|^2$ spectrum and due to the angular cuts its acceptance is smaller acceptance than that of the $|F_2|^2$ term. One then obtains the following 95% C.L. limit using the likelihood curve of fig. 3(b) and including systematic errors

$$-0.068 < F_2 < 0.065 \quad . \quad (7)$$

Discussion and Conclusions

We have studied the reaction $e^+e^- \rightarrow \tau^+\tau^-\gamma$ to search for a contribution from the anomalous magnetic form factor F_2 that is related to the anomalous magnetic moment a_τ of the τ lepton. The contribution of the F_2 form factor changes the distributions of the kinematic variables of the final state, most notably the photon energy spectrum. No significant contribution in addition to the Standard Model prediction is needed to describe the data. Comparing the data to the Standard Model prediction, a 95% confidence level limit on the magnitude of the magnetic form factor F_2 of

$$|F_2| < 0.067 \quad (8)$$

has been placed. Taking into account the effect of the interference term between the Standard Model amplitude and the F_2 amplitude the 95% CL boundary on F_2 is

$$-0.068 < F_2 < 0.065 \quad . \quad (9)$$

Substituting $\frac{F_2}{2m_\tau} \rightarrow \frac{F_3}{e}$ the bounds on F_2 translate to limits on F_3 , the electric dipole form factor of the τ lepton, for which one obtains²

$$-3.8 \times 10^{-16} e \text{ cm} < eF_3 < 3.6 \times 10^{-16} e \text{ cm} \quad , \quad (10)$$

with the same interpretation restrictions as mentioned for F_2 in the introduction and neglecting a possible influence of the τ polarization on the term linear in F_3 .

Appendix

The formulae for the differential cross section [15] for $e^+e^- \rightarrow \tau^+\tau^-\gamma$ are given below using the F_1 (SM) and the F_2 terms in the amplitude of eq.(4), but no interference.

$$\left. \begin{aligned} p_1 &= \frac{\sqrt{s}}{2} (1, 0, 0, 1) \\ p_2 &= \frac{\sqrt{s}}{2} (1, 0, 0, -1) \end{aligned} \right\} \Rightarrow p_{\text{tot}} = p_1 + p_2 = \sqrt{s} (1, 0, 0, 0)$$

²A compilation of recent bounds on electric and weak dipole moments of the τ lepton can be found in [3, 22].

$$q = E_\gamma (1, \sin \theta_\gamma \cos \phi_\gamma, \sin \theta_\gamma \sin \phi_\gamma, \cos \theta_\gamma)$$

$$k_1 = E_{\tau^-} (1, \hat{x} \sin \theta_{\tau^-} \cos \phi_{\tau^-} + \hat{y} \sin \theta_{\tau^-} \sin \phi_{\tau^-} + \hat{z} \cos \theta_{\tau^-})$$

$$k_2 = p_{\text{tot}} - q - k_1$$

$$Q^\mu = (k_1 \cdot q) k_2^\mu - (k_1 \cdot k_2) q^\mu + (k_2 \cdot q) k_1^\mu$$

$$\hat{x} = \begin{pmatrix} -\cos \theta_\gamma \cos \phi_\gamma \\ -\cos \theta_\gamma \sin \phi_\gamma \\ \sin \theta_\gamma \end{pmatrix} \quad \hat{y} = \begin{pmatrix} \sin \phi_\gamma \\ -\cos \phi_\gamma \\ 0 \end{pmatrix} \quad \hat{z} = \hat{q} = \begin{pmatrix} \sin \theta_\gamma \cos \phi_\gamma \\ \sin \theta_\gamma \sin \phi_\gamma \\ \cos \theta_\gamma \end{pmatrix}$$

$$\begin{aligned} \frac{d\sigma (e^+e^- \rightarrow \tau^+\tau^-\gamma)}{dE_{\tau^-} dE_\gamma d\cos \theta_\gamma d\phi_{\tau^-} d\phi_\gamma} &= \frac{\alpha^3}{2\pi^2 \sin^4 \theta_W \cos^4 \theta_W} \cdot \frac{1}{(s - M_{Z^0})^2 + (M_{Z^0} \Gamma_{Z^0})^2} \\ &\left\{ (c_v^2 + c_a^2)^2 \left[\frac{2}{(k_1 q)(k_2 q)} [(k_1 k_2)(p_1 p_2) - (k_1 p_1)(k_1 p_2) - (k_2 p_1)(k_2 p_2)] + \frac{(k_1 q)}{(k_2 q)} + \frac{(k_2 q)}{(k_1 q)} \right] \right. \\ &\quad \left. + 4 c_v^2 c_a^2 \left[2 \frac{(k_1 p_2)(k_2 p_1) - (k_1 p_1)(k_2 p_2)}{(k_1 q)(k_2 q)} + q (p_2 - p_1) \left(\frac{1}{(k_1 q)} - \frac{1}{(k_2 q)} \right) \right] \right\} \\ &\quad + \mathbf{F}_2^2 \cdot \frac{\alpha^3}{\pi^2 m_\tau^2 \sin^4 \theta_W \cos^4 \theta_W} \cdot \frac{1}{s [(s - M_{Z^0})^2 + (M_{Z^0} \Gamma_{Z^0})^2]} \\ &\quad \left\{ (c_a^4 - c_v^4) \left(\frac{(p_1 Q)(p_2 Q)}{(k_1 q)(k_2 q)} + (k_1 k_2)(p_1 p_2) \right) \right. \\ &\quad \left. + 2 c_v^2 (c_v^2 + c_a^2)^2 [(k_1 p_2)(k_2 p_1) + (k_1 p_1)(k_2 p_2)] \right. \\ &\quad \left. + 4 c_v^2 c_a^2 [(k_1 p_2)(k_2 p_1) - (k_1 p_1)(k_2 p_2)] \right\} \quad (11) \end{aligned}$$

Acknowledgments

This work has benefited much from numerous discussions with Dieter Zeppenfeld who has also calculated the cross section for the anomalous photon production. We would like to thank him as well as J. Biebel and T. Riemann for providing the calculations for the interference term. We would also like to acknowledge useful discussions with J. Swain, L. Taylor and O. Nachtmann.

Furthermore we particularly wish to thank the SL Division for the efficient operation of the LEP accelerator at all energies and for their continuing close co-operation with our experimental group. We thank our colleagues from CEA,

DAPNIA/SPP, CE-Saclay for their efforts over the years on the time-of-flight and trigger systems which we continue to use. In addition to the support staff at our own institutions we are pleased to acknowledge the
Department of Energy, USA,
National Science Foundation, USA,
Particle Physics and Astronomy Research Council, UK,
Natural Sciences and Engineering Research Council, Canada,
Israel Science Foundation, administered by the Israel Academy of Science and Humanities,
Minerva Gesellschaft,
Benozziyo Center for High Energy Physics,
Japanese Ministry of Education, Science and Culture (the Monbusho) and a grant under the Monbusho International Science Research Program,
German Israeli Bi-national Science Foundation (GIF),
Bundesministerium für Bildung, Wissenschaft, Forschung und Technologie, Germany,
National Research Council of Canada,
Research Corporation, USA,
Hungarian Foundation for Scientific Research, OTKA T-016660, T023793 and OTKA F-023259.

References

- [1] E.R. Cohen, B.N. Taylor, *Rev. of Mod. Phys.* **59** (1987) 1121.
- [2] E.R. Cohen, B.N. Taylor, *J. of Phys. and Chem. Ref. Data* **2** (1973) 663.
- [3] Particle Data Group, R.M. Barnett et al., *Phys. Rev.* **D54** (1996) 1.
- [4] M.A. Samuel, G. Li, R. Mendel, *Phys. Rev. Lett.* **67** (1991) 668.
- [5] F. Hamzeh, N.F. Nasrallah, *Phys. Rev.* **B373** (1996) 211.
- [6] R. Escribano, E. Masso, *Phys. Lett.* **B301** (1993) 419.
- [7] J.A. Grifolz, A. Mendez, *Phys. Lett.* **B255** (1991) 611.
- [8] D.J. Silverman, G.L. Shaw, *Phys. Rev.* **D27** (1983) 1196.
- [9] J.L. Hewett, T.G. Rizzo, *Phys. Rev.* **D56** (1997) 5709.
- [10] C.T. Hill, *Phys. Lett* **B226** (1991) 419;
B.A. Dobrescu, C.T. Hill, *Comput. Phys. Commun.* **79** (1994) 503;
W.A. Bardeen, C.T. Hill, M. Lindner, *Phys. Rev.* **D41** (1990) 1647.

- [11] S. Jadach, B. Ward, Z. Wąs, *Comput. Phys. Commun.* **79** (1994) 503.
- [12] S. Jadach, J. Kühn, Z. Wąs, *Comput. Phys. Commun.* **64** (1991) 275.
- [13] E. Barberio, Z. Wąs, *Comput. Phys. Commun.* **66** (1991) 276.
- [14] J. Allison et al., *Nucl. Inst. Meth.* **A317** (1992) 47.
- [15] D. Zeppenfeld, private communication.
- [16] S. S. Gau, T. Paul, J. Swain, L. Taylor, hep-ph/9712360 (12 Dec. 1997).
- [17] T. Sjöstrand, M. Bengtsson, *Comp. Phys. Comm.* **43** (1987) 367;
 T. Sjöstrand, *Comp. Phys. Comm.* **82** (1994) 74;
 R. Bhattacharya, J. Smith, G. Grammar, *Phys. Rev.* **D15** (1977) 3267;
 J. Smith, J.A.M. Vermaseren, G. Grammar, *Phys. Rev.* **D15** (1977) 3280;
 M. Böhm, A. Denner, W. Hollik, *Nucl. Phys.* **B304** (1988) 687.
- [18] OPAL Collaboration, K. Ahmed et al., *Nucl. Inst. and Meth.* **A305** (1991) 275.
- [19] OPAL Collaboration, M.Z. Akrawy et al., *Phys. Lett.* **B247** (1990) 458.
- [20] R. Barlow, Ch. Beeston, *Comp. Phys. Commun.* **77** (1993) 219.
- [21] J. Biebel, T. Riemann, *Z. Phys.* **C76** (1997) 53.
- [22] N. Wermes, Proc. of the TAU96 Workshop, Colorado USA, 16-19 Sept. 1996, *Nucl. Phys. B* (Proc. Suppl.) **55C** (1997) 313.